Electrochemically Smart Bimetallic Materials Featuring Group 11 Metals: In-situ Conductive Network Generation and Its Impact on Cell Capacity

Final Technical Report

DE-SC0008512

Period Covered: August 15, 2012 – September 30, 2016

November 2016

Esther S. Takeuchi

Stony Brook University

Stony Brook, NY

Final Report for DE-SC0008512

a) DOE Grant No.:	DE-SC0008512 (Renewal of Grant DE-SC0002460)
Dates of the Award:	August 15, 2012 – September 30, 2016.
Recipient Institution:	Stony Brook University (SUNY)
b) Title of Award:	"Electrochemically Smart Bimetallic Materials Featuring Group 11 Metals: In-situ Conductive Network Generation and Its Impact on Cell Capacity"
PI:	SUNY Distinguished Professor Esther S. Takeuchi
co-PIs:	SUNY Distinguished Teaching Professor Kenneth J. Takeuchi
	Research Professor Amy C. Marschilok

Technical Report

Our prior results for the program "Electrochemically smart bimetallic materials featuring Group 11 metals: in-situ conductive matrix generation and its impact on battery capacity, power and reversibility" have been highly successful: 1) we demonstrated material structures which generated in-situ conductive networks through electrochemical activation with increases in conductivity up to 10,000 fold, 2) we pioneered in situ analytical methodology to map the cathodes at several stages of discharge through the use of Energy Dispersive X-ray Diffraction (EDXRD) to elucidate the kinetic dependence of the conductive network formation, and 3) we successfully designed synthetic methodology for direct control of material properties including crystallite size and surface area which showed significant impact on electrochemical behavior. We report here results from the program (DESC0008512) organized by material class. Note that synthesis and mechanistic studies are included in each section including in-situ exploration of battery reactions.

Bimetallic vanadium phosphorous oxide materials. Polyanion compounds in the general class of MPO_4 demonstrate exceptional stability and can provide high voltage and capacity when used in lithium based batteries, but their characteristically low electrical conductivities[1-5] are one of the biggest challenges for implementation as battery materials. In order to enhance Li_xMPO_4 electrical conductivity, several strategies have emerged in the scientific literature, including coating of Li_xMPO_4 particles with carbon,[6, 7] co-synthesizing the Li_xMPO_4 materials with carbon to achieve intimate contact of the particles with the conductive material,[4, 8] adding silver and copper powder to the Li_xMPO_4 matrix to achieve improved conductivity,[9, 10] or the solid-solution doping of $LiFePO_4$.[11] However, the strategies involving the addition of an external conducting material require additional processing steps and can significantly reduce energy density due to the presence of the extraneous inert conducting material.

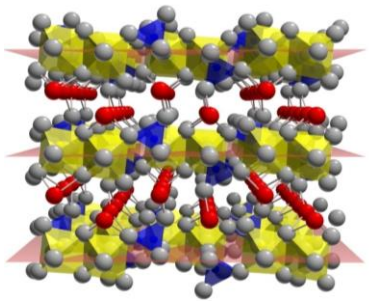

Figure 1. $Ag_2VO_2PO_4$ structure

We hypothesized that the formation of electrically conducting metal particles upon metal ion center reduction might result in an enhancement of electrical conductivity of the material, which should address conductivity problems for poorly conducting materials. Thus, we identified silver vanadium phosphorous oxides ($Ag_wV_xP_yO_z$) as a material family of interest for next generation batteries, based on the desire to obtain the chemical stability observed in phosphate cathode materials, achieve multiple electron transfer inherent in bimetallic materials, and provide the opportunity for the in-situ generation of a conductive silver matrix. We reported the first example of this strategy applied to the MPO_4 class of materials, specifically $Ag_2VO_2PO_4$,[12-15] and have affirmed this hypothesis with three other members of this material class, $Ag_{0.48}VOPO_4$,[16, 17] $Ag_2VP_2O_8$,[18-20] and $Ag_{3.2}VP_{1.5}O_8$.[21]

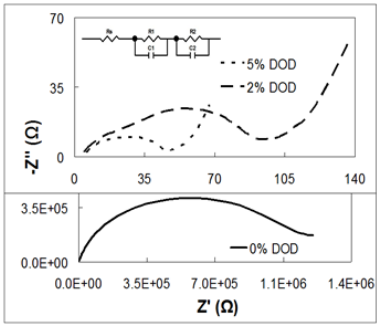

Figure 2. ACI of Li/$Ag_2VO_2PO_4$

$Ag_2VO_2PO_4$. The first member of this material family, $Ag_2VO_2PO_4$ consists of layers of dimers of edge sharing VO octahedral and PO tetrahedra, extending parallel to the (001) crystallographic plane, **Figure 1**. The Ag^+ cations reside in interlayer positions, allowing for their mobility along the VOPO layers. As a cathode material, $Ag_2VO_2PO_4$ displays several notable electrochemical properties: large capacity and an effective delivery of high current pulses. The cells supported pulsing > 40 mA/cm^2 above 2.0 V with a capacity >270 mAh/g, demonstrating 4 electrons transferred per formula unit ($Ag^+ \rightarrow Ag^o$ and $V^{5+} \rightarrow V^{3+}$).

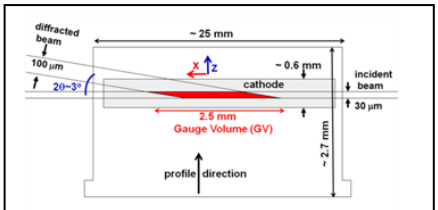

Figure 3. Diffraction geometry used for EDXRD measurement

$$Ag_2VO_2PO_4 \xrightarrow{y\text{Li } (y \le 2)} Li_xAg_{2-y}VO_2PO_4 + yAg^0$$

$$\xrightarrow{z\text{Li } (2 < z \le 4)} Li_2VO_2PO_4 + 2Ag^0$$

Ex-situ SEM and EDS analysis of partially discharged cathodes verified formation of silver nanoparticles, while XRD and XAS affirmed formation of metallic silver.[12, 14] The impact of the formation of silver metal on an $Ag_2VO_2PO_4$ cathode in a cell was studied by the use of AC impedance (ACI).[12, 13] Initially, cells with no conductive additives in the cathode showed cell resistance levels of 10^6 ohms. On reduction to 2% depth of discharge and then 5% depth of discharge the resistance decreased to 100 and then 50 ohms, **Figure 2**. This remarkable 10,000 fold increase in $Ag_2VO_2PO_4$ conductivity supported our original hypothesis.

Full understanding of the electrochemical processes taking place in batteries continues to be elusive due to the multiplicity and complex natures of the reactions associated with discharge and charge processes, and the difficulties of analytical interrogation of these reactions. A direct approach to the interrogation of the reactions taking place inside batteries is to employ in-situ strategies. Unfortunately, in-situ measurements are often hindered by diminution of signal due to the housing of an electrochemical cell or by the need to create special housings that enable the measurement. We presented an energy dispersive x-ray diffraction (EDXRD) analysis powerful enough to penetrate steel housings and thus enable in-situ study of lithium based cells and reported the first description of this technique being applied within lithium anode cells to probe a critical chemical reaction.[15] In contrast to standard top down or transmission mode XRD

methods which probe either the surface or the full sample thickness, the EDXRD technique allows interrogation of the electrode cross-section as a function of depth enabling "tomographic" profiling of the electrochemical phase changes in unmodified assembled electrochemical cells, **Figure 3**. The formation of silver metal upon the reduction of $Ag_2VO_2PO_4$ could be clearly seen at the electrode-electrolyte interface with identification of the chemical reaction front within the electrode, **Figure 4**, yielding locational information within an active battery. *This is the first report of EDXRD investigation of a lithium anode cell.*

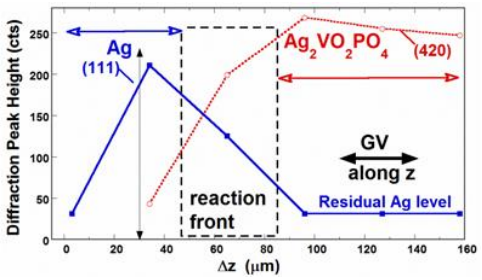

Figure 4. Peak intensity as a function of cathode location, partially discharged

$Ag_2VP_2O_8$. We reported the first electrochemical study of a silver vanadium diphosphate, $Ag_2VP_2O_8$,[18] where three electrons per formula unit were incorporated above >1.5 V.

$$Ag_2VP_2O_8 + xLi \rightarrow yLi_xAg_{2-x}V^{4+}P_2O_8 + (1-y)Li_xAg_{2-x}V^{3+}P_2O_8 + xAg^0$$

Our synthesis of $Ag_2VP_2O_8$ with a P21/c space group and structure formed by layers of VPO_8 chains comprised of VO_6 octahedra and PO_4 tetrahedra was confirmed by Rietveld refinement. Consistent with our hypothesis, the rigid diphosphate anion structure resulted in high thermal stability (>500^{0}C), boding well for enhanced safety of batteries incorporating this material. Reminiscent of $Ag_2VO_2PO_4$ reduction, in-situ formation of silver metal nanoparticles was observed with reduction of $Ag_2VP_2O_8$, discernable by XRD and SEM. However, counter to $Ag_2VO_2PO_4$ reduction, $Ag_2VP_2O_8$ demonstrated a significant decrease in conductivity upon continued electrochemical reduction with concominent fracturing of the reduced active material.

As the $Ag_2VP_2O_8$ is reduced, silver metal forms to generate a conductive network. We designed an experiment to utilized EDXRD permitting tomography-like measurements of intact Li/$Ag_2VP_2O_8$ cells at multiple depths of discharge (0, 0.1, and 0.5 electron equivalents) to visualize the formation of the conductive network.[19] In this case, determining the position and homogeneity of the conducting silver nanoparticles provides the opportunity for keen insight into the factors that limit the discharge rate in lithium based batteries, including limitation of local electronic conductivity. The determination of these factors is integral to improving performance. $Ag_2VP_2O_8$ is a good model system of a non-conducting material with the special capability of forming its own conductive pathways in-situ. Since silver metal is a high Z reduction product which can be tracked by diffraction, the spatial location of the conductive pathways can be identified as they form, providing unique insight into the discharge mechanism.

The results of the EDXRD experiment are summarized in **Figure 5**. Ag^0 was present on side of the cathode facing the Li anode at all three depths of discharge (0, 0.1, 0.5 electron equivalents), with lowest intensity in the not-discharged cell and highest intensity in the 0.5 electron equivalent cell. This is most apparent in the intensity at the Ag(111) peak position, in **Figure 5 (d, e, f)**. Based on our estimates, at 0.1 electron equivalents, ~1.1% Ag^0 is present by volume, exceeding the minimum percolation threshold of 0.3% indicating that sufficient Ag metal forms upon partial reduction of $Ag_2VP_2O_8$ to create a conducting percolation network through the cathode causing or contributing to the observed decrease in impedance providing that the spatial location of the silver was appropriate. Notably, the EDXRD data provided conclusive evidence of non-uniform discharge of the material, as evidenced by non-uniform Ag^0 and $Ag_2VP_2O_8$ intensity distributions.

Interestingly, in the 0.1 and 0.5 electron equivalent cells, the presence of silver metal also can be observed on the side of the cathode facing the cell housing (not facing the anode**), Figure 5 (e, f)**. These results affirm significant discharge of the active cathode material near the cell housing acting as a current collector. This provided evidence that the availability of electrons in addition to Li ions is a significant factor in the discharge of poorly conducting materials. The bulk $Ag_2VP_2O_8$ cathode is an insulator with high resistance, manifesting in high measured impedance (R_{ct} > 1 MΩ), **Figure 6**. Upon initiation of discharge, Ag^0 is formed on the cathode, on the side adjacent to the cell housing as well as the side facing the lithium anode, resulting in > 700X decrease in R_{ct} upon 0.1 electron equivalent of reduction. With increasing discharge to 0.5 electron equivalents, 3X further decrease in R_{ct} is observed, consistent with formation of Ag^0 throughout the thickness of the discharged cathode as is noted by the EDXRD results.

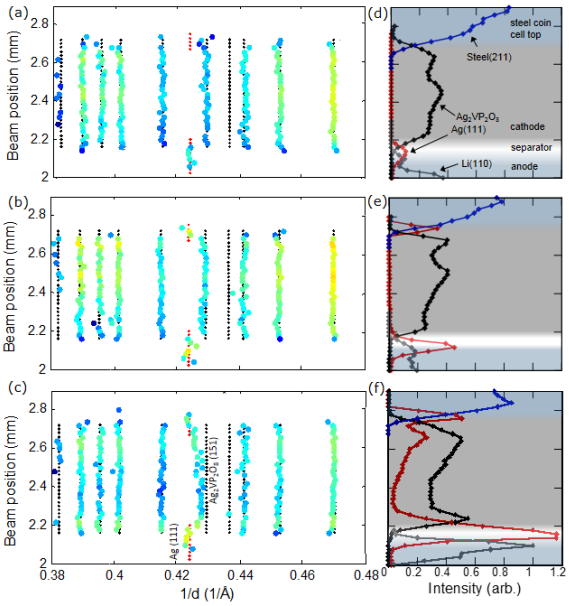

Figure 5. Li/$Ag_2VP_2O_8$ electrochemical cells discharged to (a,d) 0, (b,e) 0.1, and (c,f) 0.5 electron equivalents. Beam position vs 1/d for (a, b, c). Peak positions are represented by circles, high intensity red and low blue. Diamonds are positions for $Ag_2VP_2O_8$ (black), Li (grey), and Ag (red). Intensity of $Ag_2VP_2O_8$ and Ag^0 as a function of beam position for (d, e, f). Steel(211) - blue, Li(110) - grey, Ag(111) - red and $Ag_2VP_2O_8$ - black

We were recently able to reveal a revealing rate dependent discharge mechanism for Li/$Ag_2VP_2O_8$ cells using in-situ visualization of active batteries via EDXRD leading to a publication in *Science*.[20] Test batteries were discharged under several rates where the fastest (C/168, 7 day) discharge rate was used to provide a condition with notable evidence of polarization, while the slower (C/608, 25 day; C/1440, 60 day) discharge rates were used to provide conditions with reduced polarization. Electrochemical impedance spectroscopy (EIS) was used to probe the cell resistance, **Figure 6**. Upon partial discharge (0.5 electron equivalents), the value of R_{ct} decreases by more than three orders of magnitude, from ~1 MΩ in the not discharged cell to < 10 kΩ for the cells discharged at C/168 and C/1440. However, when comparing the fast- (C/168) and slow- (C/1440) discharged cells, R_{ct} is 3x higher in the faster rate cell at the same discharge level, indicating significantly higher impedance resulting from the faster discharge.

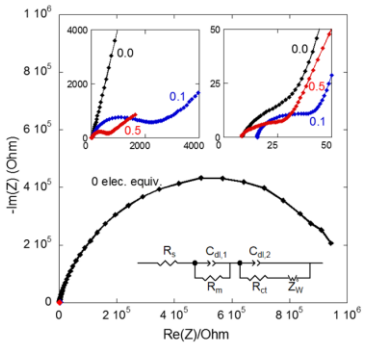

Figure 6. Impedance of Li/ $Ag_2VP_2O_8$ with initial discharge.

The use of in-situ EDXRD provided insight into the differences noted electrochemically. The non-discharged cell shows a uniform diffraction pattern throughout the cathode thickness, **Figure 7(a)**, with differences apparent only in the first scan (Ag(111) peak apparent at 1/d = 0.4239 Å) indicating formation of some Ag^0 on the cathode surface at the side opposing the anode.[19] The spectra for the two positions in the slower-discharged cell (**Figure 7(b)** and **(c)**) are similar and the Ag(111) peak intensity at 1/d = 0.4239 Å relative to the intensity of the $Ag_2VP_2O_8$ peaks is also similar between the two positions. In contrast, at the faster discharge rate (C/168), the intensity of the Ag(111) peak varies greatly among the three positions. At position 1 (**Figure 7(d)**),

the intensity of the Ag peak is larger than at positions 2 (**Figure 7(e)**) and 3 (**Figure 7(f)**). To further clarify this point, the intensities of several characteristic peaks as a function of beam position along the z-direction were determined, **Figure 8**.

Thus, two different reduction processes for the multifunctional bimetallic $Ag_2VP_2O_8$ cathode material become apparent: Ag^+ ions exit the structure and are reduced to Ag^0, and V^{4+} is reduced to V^{3+}. Although at all discharge rates both reduction processes occur, the ratio of the reduction of silver to that of vanadium changes with discharge rate where the reduction of Ag^+ is favored by slower discharge rates. The spatial distribution of Ag^0 is even in the cell discharged at the slower rate, indicating a comparatively even discharge throughout the cathode, with uniform Ag^0 concentration and consistent Ag^0 crystallite size. In the cell discharged at the faster rate, non-uniform reduction is observed with regions of higher and lower local Ag^0 content, leading to more and less favorable electron conduction pathways through the thickness of the cathode. Upon further discharge, reduction will continue to occur preferentially at these favorable locations with enhanced electron access, with incomplete utilization under high rate discharge as a consequence. *These observations provide a path to tune the electrical conductivity of cathode capable of forming conductive networks by deliberate selection of the initial discharge parameters.*

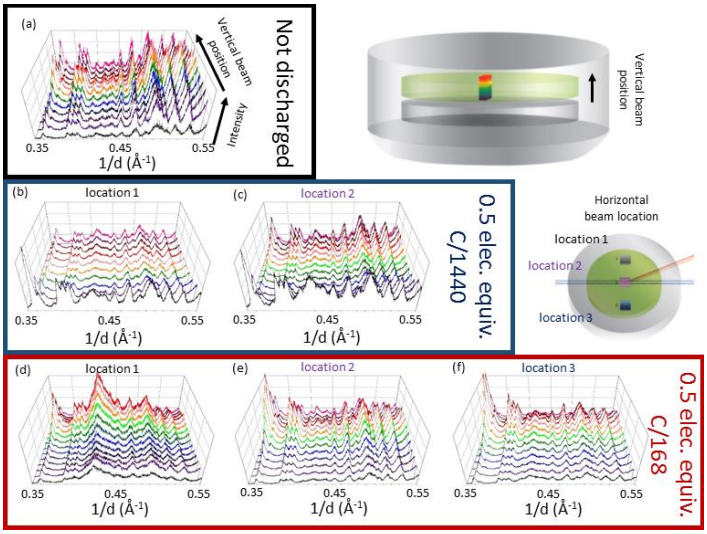

Figure 7. Experimental setup and EDXRD spectra from in-situ measurements on coin cells: (a) not-discharged, (b - c) two locations for a cell discharged to 0.5 elect. equiv. at C/1440, (d – f) three locations for 0.5 elec. equiv. at C/168.

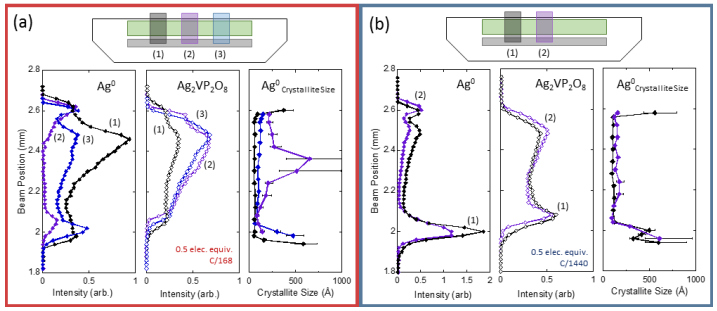

Figure 8. Intensities of Ag and $Ag_2VP_2O_8$, and crystallite size of Ag as a function of beam position along the z-direction. **A.** Cathode discharged to 0.5 electron equivalents at C/168. Three x-direction locations were measured (see schematic inset). **B.** Cathode discharged to 0.5 electron equivalents at C/1440. Two locations along the x-direction were measured in this cell.

$Ag_{3.2}VP_{1.5}O_8$. We reported the first study of the electrochemical reduction of a high Ag/V ratio silver vanadium phosphorous oxide, $Ag_{3.2}VP_{1.5}O_8$.[21] The initial reduction process involves the reduction of Ag^+ with the *in-situ* formation of silver metal nanoparticles. Upon reduction by 1 molar electron equivalent, associated conductivity increases of 9 orders of magnitude are observed. $Ag_{3.2}VP_{1.5}O_8$ demonstrates high voltage and high discharge capacity, with 175 mAh g^{-1} (~3.6 electron

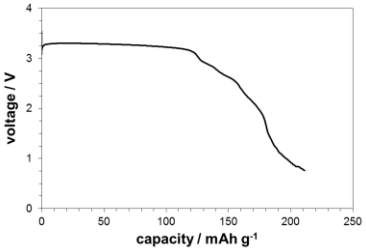

Figure 9. Constant current discharge of Li/$Ag_{3.2}VP_{1.5}O_8$

equivalents) delivered at > 2 V and ~ 125 mAh g^{-1} delivered at > 3 V, **Figure 9**. The proposed discharge mechanism is summarized as:

$$Ag_{3.2}VP_{1.5}O_8 \xrightarrow{xLi\ (x \le 2.0)} Li_xAg_{3.2-x}VP_{1.5}O_8 + xAg^0$$

$$Li_xAg_{3.2-x}VP_{1.5}O_8 \xrightarrow{yLi\ (2.0 \le y \le 3.0)} Li_{x+y}Ag_{3.2-x,y}VP_{1.5}O_8 + (x,y)Ag^0$$

$$Li_{x+y}Ag_{3.2-x,y}VP_{1.5}O_8 + x,yAg^0 \xrightarrow{zLi\ (z \le 4.5)} Li_{x+y++z}VP_{1.5}O_8 + x,yAg^0$$

The progression of the reduction of $Ag_{3.2}VP_{1.5}O_8$ is reminiscent of the reduction of $Ag_2VO_2PO_4$ where the reduction of Ag^+ to Ag^0 is the favored initial process.[12, 13] Notably, the total delivered capacity above a voltage of 3.0 V was the largest for cells with $Ag_{3.2}VP_{1.5}O_8$ cathodes among the $Ag_wV_xP_yO_z$ material series. Thus, the combination of increased conductivity early in the discharge, significant delivered capacity above 3.0 V and good pulse performance indicate promising performance attributes for $Ag_{3.2}VP_{1.5}O_8$ based cells. In addition to its high operating voltage, additional interest in the $Ag_{3.2}VP_{1.5}O_8$ is motivated by consideration of its cyclic voltammetry data where similar to $Ag_{0.48}VOPO_4 \cdot 1.9H_2O$,[22] the $Ag_{3.2}VP_{1.5}O_8$ material exhibits quasi-reversible behavior on cycle 1, with more reversible behavior on cycle 2, **Figure 10**. Further investigation of rechargeability will be the subject of a future study.

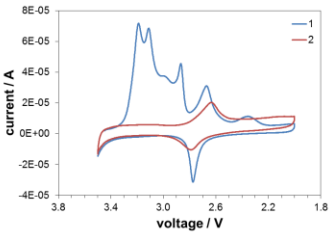

Figure 10. Cyclic voltammetry of Li/$Ag_{3.2}VP_{1.5}O_8$

Copper vanadium phosphorous oxide, $Cu_{0.5}VOPO_4 \cdot 2H_2O$. We reported the first electrochemical investigation of $Cu_{0.5}VOPO_4 \cdot 2H_2O$ as a cathode in a lithium based battery.[23] Comparison with the structure of silver vanadium phosphorous oxide, $Ag_{0.43}VOPO_4 \cdot 2H_2O$, also investigated under this program,[17, 24] shows several similarities, **Figure 11**. Both materials have a layered structure, with silver or copper ions (Ag^+ and Cu^{2+}) and water, H_2O, located between the V-O-P-O layers. The silver material has a larger interlayer spacing (6.53 Å) compared to the copper material (6.42 Å), which correlates with the larger size of Ag^+ (129 pm) relative to Cu^2 (87 pm).

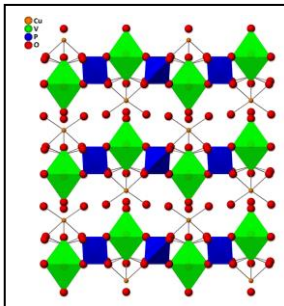

Figure 11. Structure of $Cu_{0.5}VOPO_4 \cdot 2H_2O$

Under galvanostatic discharge in lithium anode cells, $Cu_{0.5}VOPO_4 \cdot 2H_2O$ delivered ~280 mAh/g to 1.5 V. Unlike silver vanadium phosphorous oxides, crystallographic evaluation indicated little structural change upon electrochemical reduction, with no significant change in interlayer spacing and no evidence of copper metal formation. On GITT-type test, the initial polarization was large and decreased after the first 0.2 electron equivalents as the discharge progressed, **Figure 12**. On charge, the polarization increased between a reduction level of 2.0 and 1.3 electron equivalents. Subsequent to that point, the polarization decreased. The behavior during the second discharge and charge cycle was similar to the first. Notably, secondary battery evaluation showed retention of ~100 mAh/g at C/20 with little fade, a significant improvement under repeated cycling relative to the silver based material.

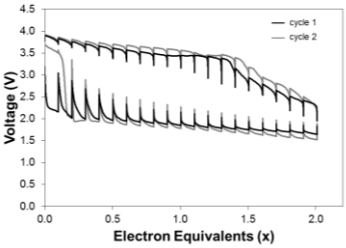

Figure 12. GITT-type test of Li/$Cu_{0.5}VOPO_4 \cdot 2H_2O$

Silver Ferrite, $AgFeO_2$. The delafossite (ABO_2) structure consists of close-packed double layers of edge-sharing BO_6 octahedra with monovalent A^+ ions positioned between the layers. Silver ferrite, $AgFeO_2$, exhibits a layered delafossite-type structure with the general chemical formula

ABO_2, **Figure 13**. We recently reported the first investigation of the electrochemical properties of silver ferrite ($AgFeO_2$), including its use as a cathode material in secondary lithium based batteries.[25]

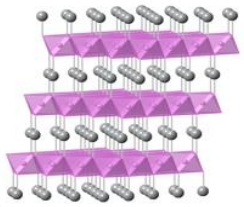

Figure 13. Structure of Ag_xFeO_2, x = 1.0

Our previous studies of crystallite size control of magnetite (Fe_3O_4) and silver hollandite ($Ag_xMn_8O_{16}$) provided fundamental crystal size / electrochemistry insight, along with a notable increase in cycling capacity with smaller crystallite size.[26-30] We hypothesized that silver ferrite crystallite size control would be possible synthetically. Further, we anticipated a crystal size / electrochemistry relationship with silver ferrite reminiscent of magnetite and silver hollandite. Silver ferrite was synthesized via a co-precipitation reaction using reagent mixture containing Ag/Fe ratios ranging between 0.2 and 1.0. XRD confirmed the structure and the relationship with crystallite size, **Figure 14.** Raman was used to probe the material and the spectra demonstrate intrinsic silver ferrite peaks while shoulders detected at 285, 374, and 707 cm^{-1} increase as the silver content decreases indicating the presence of maghemite (γ-Fe_2O_3).[31, 32] Galvanostatic cycling was conducted and the delivered discharge capacities over 50 cycles are shown, **Figure 15**. There is a significant change in capacity between cycles 1 and 2 where the change in capacity is directly proportional to the Ag^+ content in the silver ferrite when considered with respect to electron equivalents**.** Between cycles 10 and 50 the discharge capacities show only gradual fade, indicating that the discharge-charge process is reversible for this system. Notably, the silver ferrite Ag_xFeO_2 composite with the lowest silver content, x = 0.2, and smallest crystallite size delivers the highest capacity, ~200% that of stoichiometric $AgFeO_2$ and higher than maghemite alone. The critical new discovery is the direct synthesis and electrochemistry of a composite consisting of a nanocrystalline silver ferrite and an amorphous maghemite with significantly enhanced electrochemical behavior.

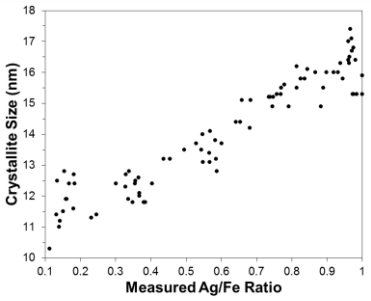

Figure 14. Crystallite size versus Ag_xFeO_2 composition

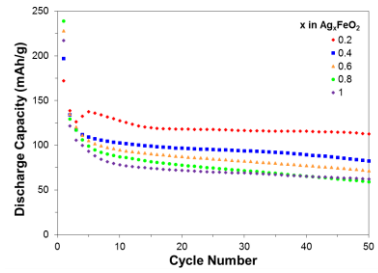

Figure 15. Discharge capacity vs. cycle number of Li/Ag_xFeO_2

Copper Manganese Oxide, Cu_xMnO_2. Manganese oxides can have diverse structures, including layered forms which can accommodate mono or divalent metal (M'^{n+}) cations along with water molecules.[33] Copper manganese oxide ($CuMnO_2$) has a layered structure consisting of edge-shared MnO_6 octahedra. A series of six $Cu_xMnO_y{\cdot}H_2O$ copper birnessite samples was prepared by varying the concentration of the Mn^{2+} precursor in the synthesis. The six $Cu_xMnO_y{\cdot}nH_2O$ samples showed an evolution in crystallite size and copper content (x) in $Cu_xMnO_y{\cdot}nH_2O$ (0.20 to 0.28) where the copper content was inversely related to crystallite size which increased with the concentration of the Mn^{2+} precursor, **Figure 16**. The small crystallite size samples delivered ~20% higher capacity than the larger size samples. XANES analysis showed that the Cu^{2+} was reduced to Cu^0 on discharge and returned to Cu^{2+} on charge indicating the possibility of reversibility of copper.

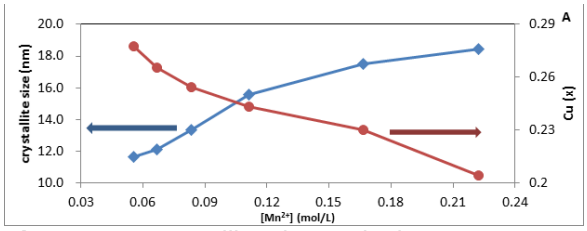

Figure 16. Crystallite size and x in $Cu_xMnO_y{\cdot}nH_2O$ as a function of Mn^{2+} precursor concentration.

Summary – Research Highlights

The research performed under this award demonstrated the profound decrease in resistance that was achievable through the appropriate design of electrochemically active bimetallic materials. Materials that are highly resistive, such as polyanion materials including $Ag_2VO_2PO_4$, increased in conductivity by 10,000 fold on initiation of reduction. This work also included pioneering use of Energy Dispersive X-ray Diffraction (EDXRD) to map the progress of a cathode reaction in a lithium anode battery, the first report of a lithium anode cell studied by EDXRD. EDXRD is a synchrotron based method for the tomographic mapping of the reaction progress through the location of the silver metal that formed in a cathode. Five publications utilizing this analytical tool resulted from the research including the identification of a rate dependent reduction mechanism for bimetallic $Ag_2VP_2O_8$, published in *Science*. A total of 18 publications resulted from the program.

Unexpended Funds. There are no unexpended funds at the conclusion of DE-SC0008512.

Publications acknowledging support from this program.

1. Kenneth J. Takeuchi, Shali Z. Yau, Melissa C. Menard, Amy C. Marschilok, and Esther S. Takeuchi, "Synthetic control of composition and crystallite size of silver hollandite, $Ag_xMn_8O_{16}$: impact on electrochemistry." ACS Applied Materials and Interfaces, 2012, 4, 5547-5554. Published
   This work was supported by the Department of Energy, Office of Basic Energy Sciences, under Grant DE-SC0002460. Galvanostatic intermittent titration-type (GITT) testing for possible use as a primary cell was supported by National Institutes of Health under Grant 1R01HL093044-01A1 from the National Heart, Lung, and Blood Institute. Rietveld analysis of the manganese compounds was funded by the New York State Energy Research and Development Authority. The authors thank Corey P. Schaffer for assistance with cyclic voltammetry measurements.

2. Amy C. Marschilok, Shali Z. Yau, Aditya Subramanian, Esther S. Takeuchi and Kenneth J. Takeuchi, "The Electrochemistry of Silver Hollandite Nanorods, $Ag_xMn_8O_{16}$: Enhancement of Electrochemical Battery Performance via Dimensional and Compositional Control." J. Electrochem. Soc, 2013, 160, (5) A3090-A3094. Published.
   This work was supported by the Department of Energy, Office of Basic Energy Sciences, under Grant DE-SC0008512. Galvanostatic discharge and galvanostatic intermittent titration-type (GITT) testing for possible use as a primary cell was supported by National Institutes of Health under Grant 1R01HL093044-01A1 from the National Heart, Lung, and Blood Institute.

3. Esther S. Takeuchi, Amy C. Marschilok, Kenneth J. Takeuchi, Alexander Ignatov, Zhong Zhong, and Mark Croft, "Energy dispersive x-ray diffraction of lithium-silver vanadium phosphorous oxide cells: In-situ cathode depth profiling of an electrochemical reduction-displacement reaction" Energy Environ. Sci., 2013, 6 (5), 1465 – 1470. Published.
   E. Takeuchi, A. Marschilok, and K. Takeuchi acknowledge support by the Department of Energy, Office of Basic Energy Sciences, under Grant DE-SC0008512.

4. Esther S. Takeuchi, Chia-Ying Lee, Po-Jen Cheng, Melissa C. Menard, Amy C. Marschilok and Kenneth J. Takeuchi, "Silver Vanadium Diphosphate $Ag_2VP_2O_8$: Electrochemistry and Characterization of Reduced Material providing Mechanistic Insights." J. Solid State Chem. 2013, 200, 232-240. Published.
   The synthesis, characterization and primary battery use studies were supported by the National Institutes of Health under Grant 1R01HL093044-01A1 from the National Heart, Lung, and Blood Institute. Mechanistic investigation of the material as a function of electrochemical reduction and assessment of reversibility were supported by the Department of Energy, Office of Basic Energy Sciences, under Grant DE-SC0002460. Rietveld analysis of the material was supported by the New York State Energy Research and Development Authority (NYSERDA), under Agreement 18517.

5. David C. Bock, Amy C. Marschilok, Kenneth J. Takeuchi, and Esther S. Takeuchi, "A Kinetics and Equilibrium Study of Vanadium Dissolution from Vanadium Oxides and Phosphates in Battery Electrolytes: Possible Impacts on ICD Battery Performance." *J. Power Sources*, 2013, 231, 219-225. Published.
   The authors acknowledge financial support for the material preparation, material characterization, and cathode solubility studies from the National Institutes of Health under Grant 1R01HL093044-01A1 from the National Heart, Lung, and Blood Institute. The authors acknowledge support for the AC impedance spectroscopy studies from the Department of Energy, Office of Basic Energy Sciences, Division of Materials Science, grant DE-SC0002460.

6. Melissa C. Menard, Amy C. Marschilok, Kenneth J. Takeuchi and Esther S. Takeuchi, "Variation in the iron oxidation states of magnetite nanocrystals as a function of crystallite size: the impact on electrochemical capacity." Electrochimica Acta, 2013, 94, 320-326. Published.
   M. C. Menard acknowledges the New York State Energy Research and Development Authority (Agreement 18517) for support of her postdoctoral fellowship. E. S. Takeuchi, K. J. Takeuchi, and A. C. Marschilok acknowledge the Department of Energy, Office of Basic Energy Sciences (Grant DE-SC0002460) for support of this project.

7. Amy C. Marschilok, Corey P. Schaffer, Kenneth J. Takeuchi, and Esther S. Takeuchi. "Carbon nanotube-metal oxide composite electrodes for secondary lithium based batteries." J. Composite Materials, 2013, 47 (1) 41-49. Published.
   The authors acknowledge the U.S. Department of Energy, Office of Basic Energy Sciences, Division of Materials Science, grant DE-SC0002460 for support related to the materials synthesis methods. The authors also acknowledge Lockheed Martin Corporation for support related to the cathode fabrication methods and electrochemical studies.

8. Esther S. Takeuchi, Amy C. Marschilok, and Kenneth J. Takeuchi, "Secondary Battery Science: At the Confluence of Electrochemistry and Materials Engineering." *Electrochemistry*, 2012, 80 (10) 700-705. Published.

Note: This was an invited Highlights Article. Thus, various sources of funding for the work that was included in the article are noted in the Acknowledgement.

Funding from the following sources is gratefully acknowledged: Department of Energy, Office of Basic Energy Sciences (Grant DE-SC0002460), National Institutes of Health, National Heart, Lung, and Blood Institute (Grant 1R01HL093044-01A1), and New York State Energy Research and Development Authority, NYSERDA, (Agreement 18517).

9. Kevin C. Kirshenbaum, David C. Bock, Zhong Zhong, Amy C. Marschilok, Kenneth J. Takeuchi, Esther S. Takeuchi. "In situ profiling of lithium/$Ag_2VP_2O_8$ primary batteries using energy dispersive X-ray diffraction," *Physical Chemistry Chemical Physics,* 2014, 16(19), 9138-9147. Published.

E. Takeuchi, K. Takeuchi, A. Marschilok and D. Bock acknowledge funding from the Department of Energy, Office of Basic Energy Sciences, under grant DE-SC0008512. Utilization of the National Synchrotron Light Source (NSLS) beamline X17B1 was supported by U.S. Department of Energy Contract DE-AC02-98CH10886. K. Kirshenbaum acknowledges Postdoctoral support from Brookhaven National Laboratory and the Gertrude and Maurice Goldhaber Distinguished Fellowship Program. The authors also acknowledge Mark C. Croft for helpful discussions.

10. Young Jin Kim, Kenneth J. Takeuchi, Amy C. Marschilok, Esther S. Takeuchi, "$Ag_{3.2}VP_{1.5}O_{7.8}$: a high voltage silver vanadium phosphate cathode material," *Journal of the Electrochemical Society,* 2013, 160(11), A2207-A2211. Published.

The synthesis, characterization, and primary battery use studies were supported by the National Institutes of Health under grant 1R01HL093044-01A1 from the National Heart, Lung, and Blood Institute. Mechanistic investigation of the material as a function of electrochemical reduction and assessment of reversibility were supported by the Department of Energy, Office of Basic Energy Sciences, under grant DE-SC0008512. The authors acknowledge Chia-Ying Lee for assistance with scanning electron microscopy.

11. Melissa C. Menard, Kenneth J. Takeuchi, Amy C. Marschilok, Esther S. Takeuchi, "Electrochemical discharge of nanocrystalline magnetite: structure analysis using X-ray diffraction and X-ray absorption spectroscopy," *Physical Chemistry Chemical Physics,* 2013, 15(42), 18539-18548. Published.

Use of the National Synchrotron Light Source, Brookhaven National Laboratory, was supported by the U.S. Department of Energy, Office of Science, Office of Basic Energy Sciences, under Contract No. DE-AC02-98CH10886. M.C. Menard acknowledges the New York State Energy Research and Development Authority (Agreement 18517) for support of her postdoctoral fellowship. E. S. Takeuchi, K. J. Takeuchi, and A. C. Marschilok acknowledge the Department of Energy, Office of Basic Energy Sciences (Grant DE-SC0002460) for support of this project. The authors acknowledge Dr Kaumundi Pandya for

helpful discussions related to Beamline X11B at the National Synchrotron Light Source at Brookhaven National Laboratory.

12. Kevin Kirshenbaum, David C. Bock, Zhong Zhong, Kenneth J. Takeuchi, Amy C. Marschilok, Esther S. Takeuchi, “In-situ visualization of Li/$Ag_2VP_2O_8$ batteries revealing rate dependent discharge mechanism,” *Science,* **2015**, 347, 149-154. Published.

    E. Takeuchi, K. Takeuchi, A. Marschilok and D. Bock acknowledge funding from the Department of Energy, Office of Basic Energy Sciences, under grant DE-SC0008512. Utilization of the National Synchrotron Light Source (NSLS) beamline X17B1 was supported by U.S. Department of Energy Contract DE-AC02-98CH10886. K. Kirshenbaum acknowledges Postdoctoral support from Brookhaven National Laboratory and the Gertrude and Maurice Goldhaber Distinguished Fellowship Program. The authors also acknowledge Mark C. Croft for helpful discussions and Yelana Belyavina for assistance with the conceptual schematics shown in Figure 1.

13. Matthew Huie, Esther S. Takeuchi, Amy C. Marschilok, and Kenneth J. Takeuchi, “Synthetic Strategies Impacting Voltage, Capacity, and Current Capability of Energy Storage Materials,” ECS Trans. 2014 61(18): 15-21; doi:10.1149/06118.0015ecst. Published.

    E. Takeuchi, K. Takeuchi, and A. Marschilok acknowledge funding from the Department of Energy, Office of Basic Energy Sciences, under grant DE-SC0008512. Pulse testing of materials in primary batteries was supported by the National Institutes of Health under grant 1R01HL093044-01A1 from the National Heart, Lung, and Blood Institute.

14. Alexander Brady, Esther S. Takeuchi, Amy C. Marschilok, and Kenneth J. Takeuchi,” Synchrotron Enabled Ex-situ and In-situ Mechanistic Interrogation of Energy Storage Systems,” *ECS Trans. 2014 61(18): 1-8; doi:10.1149/06118.0001ecst.* Published.

    E. Takeuchi, K. Takeuchi, and A. Marschilok acknowledge funding from the Department of Energy, Office of Basic Energy Sciences, under grant DE-SC0008512 covering in-situ and ex-situ mechanistic studies. Synthesis of the silver vanadium phosphate materials for primary batteries was supported by the National Institutes of Health under grant 1R01HL093044-01A1 from the National Heart, Lung, and Blood Institute.

15. Jessica L. Durham, Kevin Kirshenbaum, Esther S. Takeuchi, Amy C. Marschilok, Kenneth J. Takeuchi*, “Synthetic control of composition and crystallite size of silver ferrite composites: profound electrochemistry impacts,” Chem. Comm. 2015, 51(24), 5120-5123. Published.

    The authors acknowledge the Department of Energy (DOE), Office of Basic Energy Sciences (BES), under Grant DE-SC0008512. K. Kirshenbaum acknowledges the Gertrude and Maurice Goldhaber Distinguished Fellowship Program. X-ray absorption spectra were collected on beam line X11A at Brookhaven National Laboratory’s National Synchrotron Light Source (NSLS), supported by the DOE, Office of Science, BES, under

Contract No. DE-AC02-98CH10886. The authors acknowledge K. Pandya for assistance with XAS.

16. Esther S. Takeuchi*, Young Jin Kim, Jianping Huang, Amy C. Marschilok*, Kenneth J. Takeuchi*, “Electrochemistry of $Cu_{0.5}VOPO_4$ center dot 2H(2)O: A Promising Mixed Metal Phosphorous Oxide for Secondary Lithium based Batteries,” *J. Electrochem. Soc.,* **2015,** *162(3),* A295-A299. Published.

    The synthesis, characterization, study as a secondary battery material, and mechanistic investigation of the material as a function of electrochemical reduction were supported by the Department of Energy, Office of Basic Energy Sciences, under grant DE-SC0008512. Primary battery use studies evaluating pulse performance were supported by the National Institutes of Health under grant 1R01HL093044-01A1 from the National Heart, Lung, and Blood Institute.

17. Kevin C. Kirshenbaum, Melissa C. Menard, Young Jin Kim, Amy C. Marschilok*, Kenneth J. Takeuchi*, Esther S. Takeuchi*, “Electrochemical reduction of $Ag_{0.48}VOPO_4$: A mechanistic study employing x-ray absorption spectroscopy and x-ray powder diffraction,” J. Electrochem. Soc., 2015, 162(8), A1537-A1543. Published.

    The authors acknowledge the Department of Energy (DOE), Office of Basic Energy Sciences (BES), under grant DE-SC0008512. The XAS work was done at beamline X18B, use of the National Synchrotron Light Source, Brookhaven National Laboratory, was supported by the U.S. Department of Energy, Office of Science, Office of Basic Energy Sciences, under Contract No.DE-AC02-98CH10886. K. Kirshenbaum acknowledges Postdoctoral support from Brookhaven National Laboratory and the Gertrude and Maurice Goldhaber Distinguished Fellowship Program. M.C. Menard acknowledges the New York State Energy Research and Development Authority (Agreement 18517) for support of her postdoctoral fellowship.

18. Yue Ru Li, Amy C. Marschilok*, Esther S. Takeuchi*, Kenneth J. Takeuchi*, “Synthesis of Copper Birnessite, $Cu_xMnO_y{\cdot}nH_2O$ with Crystallite Size Control: Impact of Crystallite Size on Electrochemistry,” *Journal of the Electrochemical Society*, **2016,** *163,* A281-A285. DOI: 10.1149/2.0501602jes. Published.

    The authors acknowledge support for the materials synthesis, characterization, and lithium based electrochemical evaluation by the Department of Energy, Office of Basic Energy Sciences, under grant DE-SC0008512. Support for the magnesium based electrochemical evaluation was provided by supported by the Department of Energy, Office of Electricity, administered through Sandia National Laboratories, Purchase Order #1275961. The authors also acknowledge Brookhaven National Laboratory for the SmartLab X-ray Diffractometer.

Program participants.

PI Esther S. Takeuchi (6% effort, 1% funded by program). In 2012, E. Takeuchi relocated to Stony Brook University. For three years, her summer salary was covered as part of the transition and was not charged to research grants. She led the cathode formulation, electrochemical testing and battery assessments for the target materials.

co-PI Kenneth J. Takeuchi (3% funded by the project) directed synthesis and characterization efforts and developed synthetic methods for the new materials targets.

co-PI Amy C. Marschilok (4% effort, not charged to the program) led materials characterization efforts and assisted in materials synthesis as well as battery testing. Her salary was covered as part of the transition.

All graduate students are jointly advised by Professor Amy Marschilok, Professor Kenneth J. Takeuchi and Professor Esther S. Takeuchi unless otherwise noted.

Graduate Research Assistant Jessica Durham (59% over the course of the program) PhD level graduate student in the department of chemistry. Notably, she was just awarded an International Precious Metals Institute (IPMI) graduate student award.

Graduate Research Assistant Yue Ru Li (29% over the course of the program) Ph.D. student in the department of chemistry.

Graduate Research Assistant Christina Cama (35% over the course of the program) Ph.D. student in the department of chemistry.

Graduate Research Assistant Yiman Zhang (57% over the course of the program) Ph.D. student in the department of chemistry.

Graduate Research Assistant Jianping Huang (8% over the course of the program) Ph.D. student in the department of chemistry.

Graduate Research Assistant David Bock (5% over the course of the program) Ph.D. student in the department of chemistry.

Graduate Research Assistant Christopher Milleville (5%) was a third year Ph.D. student in the department of chemistry. Christopher Milleville left graduate studies at Stony Brook due to personal family reasons in January 2013.

Graduate Research Assistant Jiefu Yin (1% over the course of the program) Ph.D. student in the department of chemistry.

Post-doctoral Research Fellow Dr. Kevin Kirshenbaum. Dr. Kirshenbaum completed a PhD in Physics at the University of Maryland. His salary is covered by Brookhaven National Laboratory and the Gertrude and Maurice Goldhaber Distinguished Fellowship Program. He contributed 10% effort towards this project for 2 years.

Graduate Research Assistant Alexander Brady is a Ph.D. student in the department of Materials Science and Engineering. Mr. Brady was supported as a Teaching Assistant.

Graduate Research Assistant Matthew Huie is a Ph.D. student in the department of Materials Science and Engineering. He was supported as a Teaching Assistant for one year. He was then supported as a National Science Foundation Graduate Research Fellow.

The following students participated as MS students and were self-supported: Po Jen Cheng, Corey Shaffer and Aditya Subramanian.

References

1. Tarascon, J.M. and M. Armand, *Issues and challenges facing rechargeable lithium batteries.* Nature, 2001. **414**(6861): p. 359-67.
2. Gaubicher, J., et al., *Li/beta -VOPO4: a new 4V system for lithium batteries.* Journal of the Electrochemical Society, 1999. **146**(12): p. 4375-4379.
3. Amine, K., H. Yasuda, and M. Yamachi, *Olivine LiCoPO4 as 4.8 V electrode material for lithium batteries.* Electrochemical and Solid-State Letters, 2000. **3**(4): p. 178-179.
4. Huang, H., S.C. Yin, and L.F. Nazar, *Approaching theoretical capacity of LiFePO4 at room temperature at high rates.* Electrochemical and Solid-State Letters, 2001. **4**(10): p. A170-A172.
5. Yang, S., et al., *Reactivity, stability and electrochemical behavior of lithium iron phosphate.* Electrochemistry Communications, 2002. **4**(3): p. 239-244.
6. Herstedt, M., et al., *Surface Chemistry of Carbon-Treated LiFePO4 Particles for Li-Ion Battery Cathodes Studied by PES.* Electrochemical and Solid-State Letters, 2003. **6**(9): p. A202-A206.
7. Ravet, N., et al., *Electroactivity of natural and synthetic triphylite.* Journal of Power Sources, 2001. **97-98**: p. 503-507.
8. Prosini, P.P., D. Zane, and M. Pasquali, *Improved electrochemical performance of a LiFePO4-based composite cathode.* Electrochimica Acta, 2001. **46**(23): p. 3517-3523.
9. Park, K.S., et al., *Surface modification by silver coating for improving electrochemical properties of LiFePO4.* Solid State Communications, 2004. **129**(5): p. 311-314.
10. Croce, F., et al., *A novel concept for the synthesis of an improved LiFePO4 lithium battery cathode.* Electrochemical and Solid-State Letters, 2002. **5**(3): p. A47-A50.
11. Chung, S.-Y., T. Bloking Jason, and Y.-M. Chiang, *Electronically conductive phospho-olivines as lithium storage electrodes.* Nat Mater, 2002. **1**(2): p. 123-8.
12. Takeuchi, E.S., et al., *Electrochemical Reduction of Silver Vanadium Phosphorus Oxide, Ag2VO2PO4: The Formation of Electrically Conductive Metallic Silver Nanoparticles.* Chem. Mater., 2009. **21**(20): p. 4934-4939.
13. Marschilok, A.C., et al., *Electrochemical reduction of silver vanadium phosphorous oxide, Ag2VO2PO4: Silver metal deposition and associated increase in electrical conductivity.* J. Power Sources, 2010. **195**(19): p. 6839-6846.
14. Patridge, C.J., et al., *An X-ray Absorption Spectroscopy Study of the Cathodic Discharge of Ag2VO2PO4: Geometric and Electronic Structure Characterization of Intermediate phases and Mechanistic Insights.* Journal of Physical Chemistry C, 2011. **115**(29): p. 14437-14447.
15. Takeuchi, E.S., et al., *Energy dispersive X-ray diffraction of lithium-silver vanadium phosphorous oxide cells: in situ cathode depth profiling of an electrochemical reduction-displacement reaction.* Energy & Environmental Science, 2013. **6**(5): p. 1465-1470.

16. Kim, Y.J., et al., *AgxVOPO4: A demonstration of the dependence of battery-related electrochemical properties of silver vanadium phosphorous oxides on Ag/V ratios.* J. Power Sources, 2011. **196**(6): p. 3325-3330.
17. Marschilok, A.C., et al., *Silver vanadium phosphorous oxide, Ag0.48VOPO4: exploration as a cathode material in primary and secondary battery applications.* J. Electrochem. Soc., 2012. **159**(10): p. A1690-A1695.
18. Takeuchi, E.S., et al., *Silver Vanadium Diphosphate Ag2VP2O8: Electrochemistry and characterization of reduced material providing mechanistic insights.* Journal of Solid State Chemistry, 2013. **200**: p. 232-240.
19. Kirshenbaum, K.C., et al., *In situ profiling of lithium/Ag2VP2O8 primary batteries using energy dispersive X-ray diffraction.* Phys Chem Chem Phys, 2014. **16**(19): p. 9138-47.
20. Kirshenbaum, K.C., et al., *In-situ visualization of Li/Ag2VP2O8 batteries revealing rate dependent discharge mechanism* Science, 2015. **347**(6218): p. 149-154.
21. Kim, Y.J., et al., *Ag3.2VP1.5O7.8: a high voltage silver vanadium phosphate cathode material.* J. Electrochem. Soc., 2013. **160**(11): p. A2207-A2211.
22. Bock, D.C., et al., *Silver vanadium oxide and silver vanadium phosphorous oxide dissolution kinetics: a mechanistic study with possible impact on future ICD battery lifetimes.* Dalton Transactions, 2013. **42**: p. 13981-13989
23. Takeuchi, E.S., et al., *Electrochemistry of Cu0.5VOPO4•2H2O: A promising mixed metal phosphorous oxide for secondary lithium based batteries.* Journal of the Electrochemical Society, 2015. **162**(3): p. A295-A299.
24. Kim, Y.J., et al., *Ag(x)VOPO(4): A demonstration of the dependence of battery-related electrochemical properties of silver vanadium phosphorous oxides on Ag/V ratios.* Journal of Power Sources, 2011. **196**(6): p. 3325-3330.
25. Farley, K.E., et al., *Synthesis and Electrochemistry of Silver Ferrite.* Electrochem. Solid-State Lett., 2012. **15**(2): p. A23-A27.
26. Takeuchi, K.J., et al., *Synthetic Control of Composition and Crystallite Size of Silver Hollandite, $Ag_xMn_8O_{16}$: Impact on Electrochemistry.* ACS Applied Materials and Interfaces, 2012. **4**: p. 5547-5554.
27. Takeuchi, K.J., et al., *The Electrochemistry of Silver Hollandite Nanorods $Ag_xMn_8O_{16}$: Enhancement of Electrochemical Battery Performance via Dimensional and Compositional Control.* Journal of the Electrochemical Society, 2013. **160**: p. A3090-A3094.
28. Zhu, S., et al., *Crystallite Size Control and Resulting Electrochemistry of Magnetite, Fe_3O_4.* Electrochemical and Solid-State Letters, 2009. **12**: p. A91-A94.
29. Zhu, S., et al., *Nanocrystalline Magnetite: Synthetic Crystallite Size Control and Resulting Magnetic and Electrochemical Properties.* Journal of the Electrochemical Society, 2010. **157**: p. A1158-A1163.
30. Menard, M.C., et al., *Variation in the Iron Oxidation States of Magnetite Nanocrystals as a Function of Crystallite Size: The Impact on Electrochemical Capacity.* Electrochimica Acta, 2013. **94**: p. 320-326.
31. Dar, M.I. and S.A. Shivashankar, *Single Crystalline Magnetite, Maghemite, and Hematite Nanoparticles with Rich Coercivity.* RSC Advances, 2014. **4**: p. 4105-4133.
32. Chaudhari, N.S., et al., *Maghemite (Hematite) Core (Shell) Nanorods via Thermolysis of a Molecular Solid of Fe-Complex.* Dalton Transactions, 2011. **40**: p. 8003-8011.
33. Ching, S., R.P. Neupane, and T.P. Gray, *Synthesis and characterization of a layered manganese oxide: Materials chemistry for the inorganic or instrumental methods lab.* J. Chem. Educ., 2006. **83**(11): p. 1674-1676.